Dispersion Polymerization in Supercritical CO_2 with a Siloxane-Based Macromonomer: 1. The Particle Growth Regime

M. L. O'Neill, M. Z. Yates, and K. P. Johnston*

Department of Chemical Engineering, The University of Texas at Austin Austin, Texas 78712-1062

C. D. Smith and S. P. Wilkinson

Air Products and Chemicals, Inc. Allentown, Pennsylvania 18195-1501

Received September 3, 1997; Revised Manuscript Received December 30, 1997

ABSTRACT: Particle growth rates were analyzed for the dispersion polymerization of methyl methacrylate (MMA) in supercritical carbon dioxide at 65 °C stabilized with a poly(dimethyl siloxane)-methyl methacrylate (PDMS-mMA) macromonomer. Although pure CO_2 is a mediocre solvent for PDMS even at 4000 psia, the monomer behaves as a cosolvent to prevent flocculation. As pressure is decreased, the dispersion flocculates sooner, as expected due to the reduced solvent quality of CO_2. Final particle size is only mildly dependent on pressure as a result of the solvation from the high monomer concentration during the particle formation stage, however particle coagulation increases with decreasing pressure. There exists both a minimum pressure (∼3000 psia) and stabilizer concentration (∼2 wt % stabilizer/monomer) below which particles are highly coagulated due to insufficient steric stabilization. Here polymerization rates are reduced due to diffusional restrictions. This threshold pressure and stabilizer concentration are required to change the mechanism from precipitation polymerization to dispersion polymerization, as indicated by product morphology, molecular weight, and molecular weight polydispersity. Final particle size and number density determined from the model of Paine {*Macromolecules* **1990**, *23*, 3109} agree with the measured values.

Introduction

The first generation of research involving surfactants in supercritical fluids (SCFs) addressed reverse micelles and water-in-SCF microemulsions, for alkanes such as ethane and propane,[1−4] as reviewed recently.[5,6] Peck and Johnston[7] developed a lattice fluid self-consistent field theory of the structure and interactions of surfaces with anchored chains in compressible solvents, including supercritical fluids. This model describes microemulsions, emulsions, and latexes. As two droplets or particles approach each other, the solvent leaves the interfacial region to increase the volume and entropy. This separation of solvent and polymer chains leads to flocculation and is analogous to phase separation between polymer chains and solvent in bulk. Acrylate emulsions stabilized by highly CO_2-philic polymer chains flocculate at the θ density of these chains based on turbidimetry[8] and dynamic light scattering measurements,[9] in accordance with the aforementioned lattice fluid self-consistent field theory.

Recent polymerization reactions have utilized supercritical CO_2 to replace more traditional solvents.[10−16] Polymer latexes in SC−CO_2 may be produced from soluble organic monomers through dispersion polymerization. These dispersions may be stabilized sterically with high molecular weight CO_2-soluble homopolymers and copolymers.[10,17] Because CO_2 has such a low dielectric constant, electrostatic stabilization does not appear to be feasible because of the very thin electrical double layer. Polymers with a low polarizability per volume and thus a low surface tension are soluble in supercritical CO_2;[18] for examples, fluoroacrylate-, fluoroether-, siloxane-, and propylene oxide-based polymers. Relatively monodisperse micron-sized particles of poly(methyl methacrylate),[12,15,16] poly(styrene),[13] and poly(2,6 dimethyl phenol)[14] have been produced by dispersion polymerization with yields of >90% and molecular weights of $>10^5$ g mol^{-1}. Recently, Lepilleur and Beckman[16] followed the overall rate of polymerization of methyl methacrylate by pressure measurements in a constant volume reactor.

In dispersion polymerization, there are many factors that affect the particle size and molecular weight, such as initiator concentration, stabilizer concentration, temperature, and solvent strength of the continuous phase. A parameter unique to dispersion polymerization in supercritical fluids is the modification of the continuous phase solvent strength through changes in pressure. Also, unlike most common organic solvents, CO_2 lacks labile hydrogens, which eliminates chain transfer to solvent as a contributor to radical termination.

A model first developed by Paine[19] utilizes aspects of free radical polymerization kinetics and theory of steric stabilization to predict final particle size and particle number density in dispersion polymerization. This method has been moderately successful for polymerizations of styrene,[19,20] butyl methacrylate,[21] and methyl methacrylate[20] in liquid media. The model describes particle formation and growth in dispersion polymerizations stabilized with macromonomers and grafting homopolymers and will be used to interpret our results.

The objective of this study is to gain insight into the mechanism of particle growth in dispersion polymerization in supercritical CO_2. A detailed study of the chronology of product yield, particle size, morphology, particle number density, and molecular weight was undertaken. The system studied was methyl methacrylate (MMA), initiated by 2,2′azobis(isobutyronitrile) (AIBN) at 65 °C. The stabilizer was a reactive poly(dimethylsiloxane) macromonomer containing a single reactive methacrylate end group (PDMS-mMA). In the first set of experiments, polymerizations were conducted

S0024-9297(97)01314-4 CCC: $15.00
Published on Web 04/17/1998

at 3000 psia, 65 °C, and ~0.25 g MMA/g CO_2 (25 wt %), 0.05 g PDMS-mMA/g MMA (5 wt %), and 0.01 g AIBN/g MMA (1 wt %). In the final two sections, similar experiments were conducted in which either the pressure (1500 to 4000 psia) or macromonomer concentration (0 to 10 wt %) was varied. The combination of visual observations of flocculation and sedimentation, phase behavior for the stabilizer at reaction conditions, and particle morphology from electron micrographs provides a detailed picture of the stabilization conditions. Rates of reaction, kinetic rate constants, loci of polymerization, and mechanisms of stabilization are reported. Finally, the experimental results are correlated with predictions of the Paine model to aid in the understanding of particle growth, particularly the relationship of particle size and molecular weight with conversion. This study of particle growth, which expands upon the previous work of Shaffer et al.,[15] complements a detailed study in part 2 of this series of the particle formation stage by in situ turbidimetry.[22]

Theory

In dispersion polymerization, the reaction mixture is initially homogeneous. At the earliest stages of polymerization, initiation and propagation occur in the solution phase, and oligomers formed are soluble in the reaction mixture. As the growing polymer chains become too large to remain solubilized, the chains nucleate and aggregate from solution to form particles. This particle formation stage is assumed to be complete relatively quickly, and the particle number density remains constant for the duration of the polymerization. Growth of existing particles proceeds by absorption of monomer, as well as by absorption of polymer chains and unstabilized polymer nuclei, leading to a relatively monodisperse product.[19,23] The small particle sizes minimize diffusional restrictions of the monomer in the particle phase and reduce thermal energy build-up.

Kinetic models of dispersion polymerization are based on bulk polymerization kinetics.[24,25] In classical free radical polymerization kinetics it is known that:[24]

$$R_i = 2 f k_d [\mathbf{I}] \quad (1)$$

where R_i is the initiation rate, k_d is the initiator decomposition rate constant, f is the initiator efficiency, and [**I**] is the initiator concentration. The values for f and k_d have been determined for AIBN in supercritical CO_2.[26] The rate of polymerization R_p is related to the monomer concentration [**M**] by:[23,27]

$$R_p = -\mathrm{d}[\mathbf{M}]/\mathrm{d}t = \mathrm{d}X/\mathrm{d}t\,[\mathbf{M}_0] \quad (2)$$

$$R_p = k_p [\mathbf{M}] (R_i/2k_t)^{1/2} = k_p [\mathbf{M}] (f k_d [\mathbf{I}]/k_t)^{1/2} \quad (3)$$

where X is the fractional conversion of monomer, R_i is the rate of initiation, [**I**] is the concentration of initiator, k_p, k_t, k_d are the propagation, termination, and initiator decomposition rate constants, respectively, and f is the initiator efficiency. In dispersion polymerization, determination of k_p from eqs 2 and 3 requires estimation of the partition coefficient of monomer between the particle and continuous phases.

In bulk polymerization, k_p has been shown to be almost constant throughout a reaction, unaffected by changes in the polymerizing medium until conversions become very high.[23,27] The value for k_t, however, decreases throughout the reaction because of the increasing viscosity of the bulk phase. This Trommsdorff or gel effect results in the rapid increase in the polymerization rate R_p proportional to $(k_p/k_t^{1/2})$, as shown in eq 3. This effect produces the sigmoidal shape frequently seen in conversion versus time profiles for bulk and dispersion polymerization.[23]

Polymer molecular weight may be described by the relationship $n = R_p/R_t$, where n is the chain length and R_t is the rate of termination.[25] As the locus of polymerization shifts from the solution phase to the particle phase, a concurrent increase in polymer molecular weight occurs due to a reduction in R_t caused by the higher viscosity of the polymer phase. Toward completion of the polymerization, dramatic increases in polymer viscosity are observed if the glass transition point for the polymer is crossed.

For grafted stabilizers, Paine's[19] model predicts final particle sizes and number densities. The final particle size, d_f, is determined by:

$$d_f = (6\mathrm{MW}_M[\mathbf{M}]/\rho N_A)^{2/3}(Q_{min}/C_S[\mathbf{S}])^{1/2} \times (k_2/0.386\pi k_p)^{1/6}(k_t/f k_d[\mathbf{I}])^{1/12} \quad (4)$$

where MW_M and [**M**] are the monomer molecular weight and concentration, ρ is the particle phase density, N_A is Avogadro's number, Q_{min} is the minimum coverage (grafts/cm^2) required to stabilize the surface area of the dispersion, C_S is the relative reactivity of the stabilizer to monomer, [**S**] is the stabilizer concentration, and k_2 is the diffusion-controlled rate constant for particle collisions. It is noteworthy that eq 4 assumes complete incorporation of the polymerized macromonomer onto the particles. For this study, the minimum surface coverage (grafts/cm^2) required for stabilization by the macromonomer is:

$$Q_{min} = 1/\pi\, R_g^{\,2} \quad (5)$$

Equation 5 assumes that the surface area occupied per stabilizer molecule is equal to the bulk stabilizer tail area based on the de Gennes "mushroom" configuration.[31]

The third factor of eq 4 accounts for the availability of the stabilizer through the chain transfer constant C_S and [**S**]. The value of C_S represents the ratio of reactivities of a macromonomer versus a monomer unit for a growing radical oligomer in the solution phase. The C_S for PDMS-mMA is influenced by the molecular weight of the PDMS tail. The value of C_S varies from as high as 1 for low molecular weight PDMS-based macromonomers (~1×10^3 g mol^{-1}) to ~0.5 for macromonomer with PDMS portions of similar molecular weight as used in this study.[32,33] The decrease in C_S with increasing stabilizer tail molecular weight has been attributed to the incompatibility between the tail material and the polymer being formed (i.e., PDMS and PMMA, respectively, in this study). It has been noted that the reduction in C_S with molecular weight is more pronounced when the continuous phase media is a preferential solvent for the stabilizer.[32,33]

Experimental Section

Materials. Methyl methacrylate (MMA), poly(dimethylsiloxane)-monomethacrylate (PDMS-mMA; ~10^4 g mol^{-1}), and 2,2′-azobis(isobutyronitrile) (AIBN) were obtained from Aldrich Chemicals and used as received.

The monomer and PDMS-mMA were purged with nitrogen (Liquid Carbonics, >99.999%) before use. Carbon dioxide was obtained from Liquid Carbonics (instrument grade, < 20 ppm oxygen) and was passed through a Labclear high-pressure oxygen trap (Oxyclear model RGP−R1−300) prior to use. The reactor was purged with CO_2 prior to reactant introduction.

Apparatus and Procedure. The polymerization experiments were conducted in a ∼2.25-mL high-pressure view cell with a miniature Teflon-coated magnetic stir bar (Fisher Microbar, 7 × 2 mm; #14−511−67) and fitted with two 2.54-cm diameter by 1.0-cm thick sapphire windows. Known amounts of PDMS-mMA and AIBN were first introduced to the cell. The cell was then purged with CO_2 at 100−200 mL/min (gas) for 10 min prior to the introduction of MMA. Once a measured amount of monomer was introduced, the cell was sealed and placed into a 60 °C water bath. The bath was heated to 65 °C, and stirring of the reactor contents commenced as the cell was introduced to the bath. The cell was slowly pressurized as the water bath approached 65 °C. Thermal equilibrium was achieved within 2 min of placing the reactor in the bath, as determined from similar measurements utilizing a thermocouple inside the reactor. The time required for the bath to reach 65 °C took ∼3 min, and it was assumed that the reactor reached 65 °C at the same time as the bath. The reactor was kept isobaric with an ISCO computer-controlled syringe pump (model 270D) and was monitored with a Sensotec pressure transducer and readout (models TJE−7039−01 and GM, respectively).

All polymerizations were initially homogeneous after placing the reactor into the heated water bath (65 °C) and pressurizing with CO_2. After reaching thermal equilibrium, 6 to 9 min passed before the contents of the reactor became turbid, which is indicative of a heterogeneous dispersion of polymer-rich particles that have phase separated from the CO_2-rich continuous phase. Phase separation was noted as the point where the cell contents began to show a faint orange tint, which is indicative of Rayleigh scattering by small particles of nucleated polymer. The incubation period prior to phase separation is the result of traces of oxygen and hydroquinone monomethyl ether (inhibitor shipped with MMA, ∼ 10 ppm) that inhibit the initiation of MMA, and the time required to produce PMMA of sufficient molecular weight to become insoluble in the CO_2/MMA continuous phase mixture.

This incubation period allowed the reaction mixture to attain thermal equilibrium before initiation of MMA commenced. As noted in previous studies,[19] the presence of inhibitor does not affect the initiation rate, but only delays the polymerization as inhibitor is consumed by initiator radicals. All reactions were compared on a time scale corrected to the onset of phase separation. Due to the insoluble nature of even 3000 molecular weight oligomers of PMMA in CO_2,[18] the onset of turbidity will correspond closely to the start of polymerization of MMA. A separate experiment was performed with monomer that was passed through an alumina column to remove inhibitor. Also, AIBN was purified through recrystallization from methanol. The solution became turbid in 6 min, similar to the aforementioned results. The final particle size of PMMA particles produced by the two techniques were the same.

Reactions were quenched at various times via rapid cooling by replacing water from the bath with ice while stirring continued. This addition of ice resulted in a reduction of the bath temperature to slightly below ambient in <1 min. After 10 min of cooling in the bath, the reactor was removed, stirring was ceased, and the sample was extracted with ∼20 mL of liquid CO_2 at the reaction pressure and ambient temperature with mild manual stirring. The extraction step removed any unreacted MMA and PDMS-mMA from the system. There were no attempts made to collect the extracts. Depressurization was done slowly over several minutes to avoid sample losses.

The majority of the PMMA particles samples were removed with a microspatula and placed into a tared glass vial. Residues were dissolved in dichloromethane, and the solution was placed in a second tared glass vial. The samples were allowed to dry for 12 h at room temperature, and then for a further 12 h at 70 °C to remove residual solvent. Yields were determined gravimetrically from the ratio of the final mass of polymer collected to initial MMA loading. Molecular weight was characterized by GPC relative to PS standards (THF @ 35 °C and 1 mL min^{-1} flow rate, 50-μL injection, ∼0.002 g mL^{-1} polymer) on a Polymer Labs 5M mixed C columns (10^6 − ∼400) with a refractive index (RI) detector. Latex morphology was analyzed and imaged with a Joel JSM-35C scanning electron microscope (SEM). Samples were sputter coated with gold−palladium to a thickness of ∼200 Å. Average sizes and polydispersities were calculated based on 25−50 particles measured from the micrographs.

The phase behavior for the macromonomer in supercritical CO_2 at 65 °C was determined in a manner very similar to that described previously.[12] A macromonomer concentration of 5 wt % PDMS-mMA/MMA at 20 wt % MMA/CO_2 was used (i.e., ∼ 1 wt % PDMS-mMA/CO_2). Phase boundaries were determined with additions of MMA from 0 to 20 wt % MMA/CO_2 to imitate continuous phase compositions in polymerizations.

Results and Discussion

Phase Behavior of PDMS-mMA Macromonomer. The phase behavior of the macromonomer in CO_2 at 65 °C is shown in Figure 1 for a concentration similar to that used in the polymerizations. The phase behavior of PDMS-mMA has been shown to be very similar to that for PDMS homopolymer of a similar molecular weight,[18] indicating little influence from the terminal methacrylate group. The addition of MMA to the CO_2 phase results in a reduction in the phase separation pressure of ∼90 psia/wt % MMA, indicating that MMA is a cosolvent for PDMS. The presence of MMA has also been shown to improve the solvation of poly(1,1-dihydroperfluorooctyl acrylate), poly(FOA), in CO_2 despite the fact that MMA is a nonsolvent for the polymer.[12]

Carbon dioxide is known to be a mediocre solvent for PDMS of similar molecular weight to that used in this study.[34] It was recently shown by emulsion stability studies that steric stabilization in supercritical CO_2 is related to the theta-point density for the "tail" of the stabilizer in the continuous phase.[8,9] The theta-point pressure (or density) of infinite molecular weight PDMS in pure CO_2 will be significantly higher than the measured phase boundary for moderate molecular weight. However, with additions of cosolvent such as MMA, the mixture may in fact become a better-than-

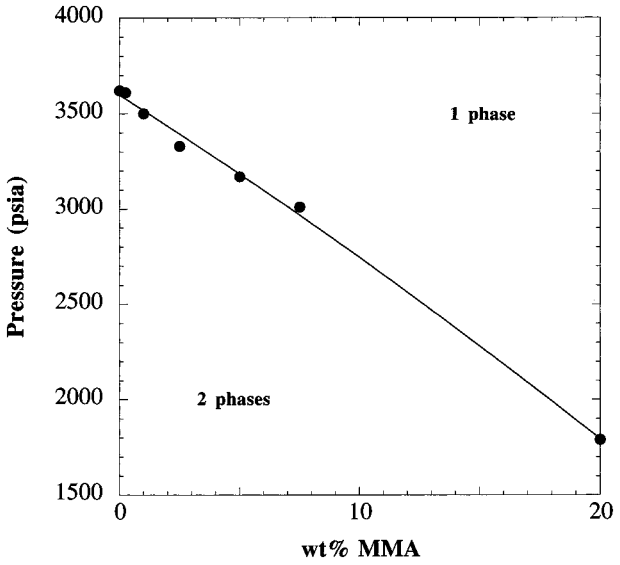

Figure 1. Cloud point pressures for ~1.2 wt % PDMS-mMA/CO_2, ~5 wt % PDMS-mMA/MMA at 65 °C. Errors in cloud point pressure are approximately ±20 psia.

theta solvent for PDMS. Throughout the polymerization, the theta-point profile for PDMS will change with MMA concentration analogously to Figure 1.

Chronology of Latex Morphology and Stabilization. A pressure of 3000 psia was used for all polymerizations discussed in this section. For all reactions quenched at times ≤1.25 h after phase separation, extraction of residual monomer was crucial to prevent coagulation of particles during depressurization. Samples collected at times ≤30 min had a coagulated morphology regardless of the amount of CO_2 used in the subsequent extraction; that is, even up to 40 mL liquid CO_2 (~ 15 residence volumes) at 3000 psia and 23 °C (Figure 2, a-b). From Table 1 it is obvious that a rather dramatic increase in particle size occurs from 15 to 30 min. In part 2,[22] we show by turbidimetry how particle coagulation is a critical part of the mechanism of particle formation during the first 5% conversion of monomer to polymer.

The latex produced for reactions quenched at times ≤1.25 h was stable for at least 5 min, as determined by visual observations after the temperature quench. Upon extraction of monomer, the latexes began to flocculate and sediment. The removal of MMA resulted in a reduction of the solvency of the continuous phase for the PDMS "tail", and a concomitant loss of stabilization against flocculation. These samples appeared spherical (Figure 2, c-d), as the flocculated particles did not have sufficient time to coalesce significantly during the extraction and subsequent depressurization steps.

In a separate set of experiments, reactions quenched after exactly 1.25 h were subjected to different extraction procedures to investigate latex stability and final product morphology. Samples left stirring for 12 h prior to extraction of MMA remained spherical and did not coagulate, as was the case for those extracted immediately following quenching. However, latexes that were first extracted and then left stirring for 12 h showed definite signs of coagulation. This comparison illustrates clearly that MMA acts as a cosolvent for PDMS in these systems.

The latexes produced at ≥2 h settled rapidly (i.e., 1 cm in <10 s) once stirring was stopped. The average size of the particles obtained from reactions quenched at 2 h was ~3.0 μm (Table 1, Figure 2, e−f). The degree of coagulation of particles increases for longer polymerization times. The sedimentation time for spherical particles may be determined from the Stokes equation, $t = (9\eta h/2\Delta\rho g r^2)$, where η is the viscosity of the continuous phase, h is distance, $\Delta\rho$ is the density difference between the particle and the continuous phase, g is the acceleration due to gravity, and r is the particle radius. Using a particle density of 1.15 g/mL for pure PMMA (the actual particle density will be slightly lower due to swelling by CO_2 and MMA), a CO_2 density of 0.9 g mL^{-1}, and viscosity of 5.8×10^{-4} Poise at 3000 psia and 25 °C, it should take on the order of 1000 s for 3.0-μm particles to settle 1 cm. As there is no indication of an increase in the size of particles remotely sufficient to account for the increased sedimentation, it is inferred that flocculation of the dispersion had occurred.

Based on the data of Figure 1, it is estimated that at least 7 to 8 wt % MMA is needed in the continuous phase to prevent flocculation of the dispersion. This amount correlates to a conversion of ~50% assuming a partition coefficient of 1 (based on volume fraction) for MMA between CO_2 and PMMA. This prediction agrees very well with the actual conversions obtained between 1.25 and 2.0 h reaction time when latex particles began to show signs of flocculation and coagulation.

Molecular Weight and Particle Size as a Function of Conversion. From Figure 3 an exponent of 0.49 is found for the dependence of the weight average molecular weight on conversion. Molecular weights approach 5×10^5 g mol^{-1}, and unlike the case for dispersion polymerizations in liquids, there is no reduction observed in molecular weight with conversion. As a result of the significant solubility of CO_2 in the polymer phase, the T_g is depressed below the reaction temperature.[28,30] With rapid monomer diffusion into the polymer phase,[35] the polymerization rate remains high essentially to completion of the polymerization, as shown previously.[12,13]

The molecular weight is lower and the polydispersities are slightly higher than in previous studies,[12,15] primarily because of the higher initiator concentration. Although inhibitors can produce chain-terminating agents and reduce conversions for vinyl acetate, little effect of this kind has been seen for MMA.[36] There was no discernible trend observed in polydispersity with reaction time.

In Figure 4, an exponent of 0.29 was determined for the dependence of size on conversion; this value is in good agreement with a value of 1/3 expected from simple geometry when conversion scales directly with particle volume.[19] Therefore, throughout the majority of the reaction, few new particles are formed. These results in combination with the high molecular weights obtained suggest that little, if any, of the polymer formed in solution coagulates with existing particles before radical termination occurs in solution and before new particles are formed through adsorption of stabilizer. The scatter in size versus conversion data results from uncertainty in sampling of the latex for the particle size (determined by SEM), and sample losses during extraction and recovery stages.

Kinetics of Dispersion Polymerization in CO_2. Reactions conducted at 3000 psia were essentially complete after 3.5 h (Figure 5). The fractional conversion rate dX/dt, determined from the maximum slope of a plot of yield versus time, was 0.83% min^{-1} at ~10−

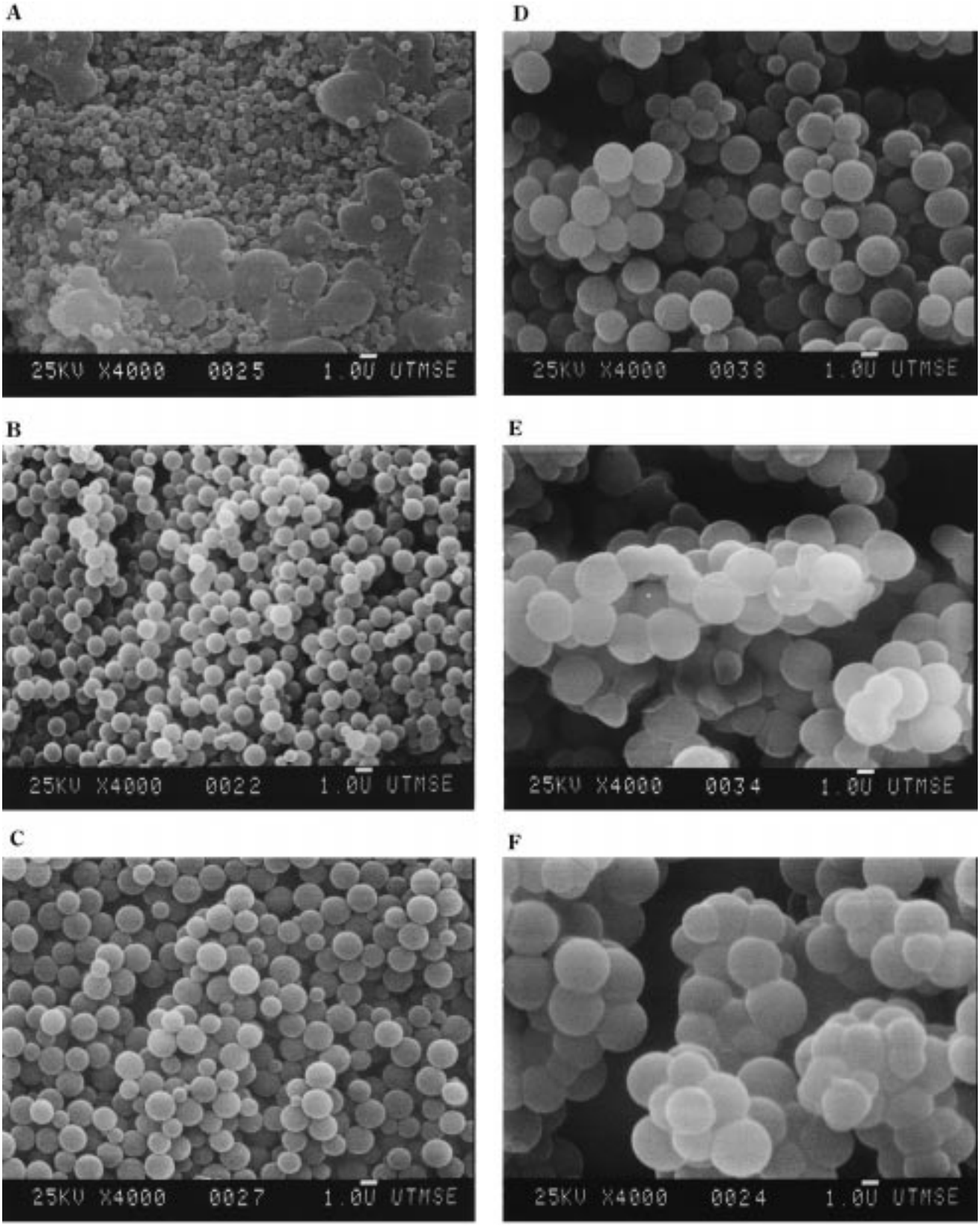

Figure 2. SEM micrographs of PMMA particles for dispersion polymerizations quenched at various times at 3000 psia and 65 °C. All micrographs are at 4000X magnification: (A) 15 min; (B) 30 min; (C) 60 min; (D) 90 min; (E) 120 min; (F) 300 min after phase separation.

20% conversion, which is in good agreement previous results.[12,16] For the first 40 min, the reaction is slow because the large reduction in k_t (the gel effect) is not yet present. To determine the propagation rate constant k_p from conversion rate data and the final particle size, accurate values for the initiator decomposition rate constant k_d, the initiator efficiency f, and the termination rate constant k_t must be known.

Initiator decomposition rate constant and efficiency of 8.6×10^{-6} s^{-1} and 0.83, respectively, have been

Table 1. Dispersion Polymerization of MMA in CO_2 Quenched at Various Times[a]

time (h)	yield (%)	M_w ($\times 10^3$ g/mol) /PDI	product morphology	approximate particle size (μm)/PDI[b]
5.0	90	409/4.1	partially coagulated	3.1/1.11
	93	339/4.0		
3.5	98	408/4.0	partially coagulated	3.1/1.07
2.0	71	341/3.6	partially coagulated	3.0/1.02
1.75	51	251/3.7	partially coagulated	2.4/1.24
1.5	36	220/6.5	partially coagulated	2.1/1.14
1.25	34	202/4.4	uncoagulated	1.8/1.16
1.1	15	170/7.1	uncoagulated	1.4/1.32
1.1	12	140/5.7	uncoagulated	1.6/1.20
1.0	18	148/3.2	uncoagulated	1.4/1.16
0.92	16	160/5.6	uncoagulated	1.6/1.08
0.67	5	70.7/4.0	uncoagulated	1.2/1.14
0.50	n/a	n/a	partially coagulated	1.1/1.10
0.50	n/a	n/a	partially coagulated	1.1/1.14
0.25	n/a	n/a	partially coagulated	0.6/1.07

[a] All samples were extracted with ~6 residence volumes of pure CO_2, all reactions were 25−30 wt % MMA/CO_2, ~5 wt % PDMS-mMA/MMA, ~1 wt % AIBN/MMA, 3000 psia, and 65 °C. [b] Weight average diameter/number average diameter.

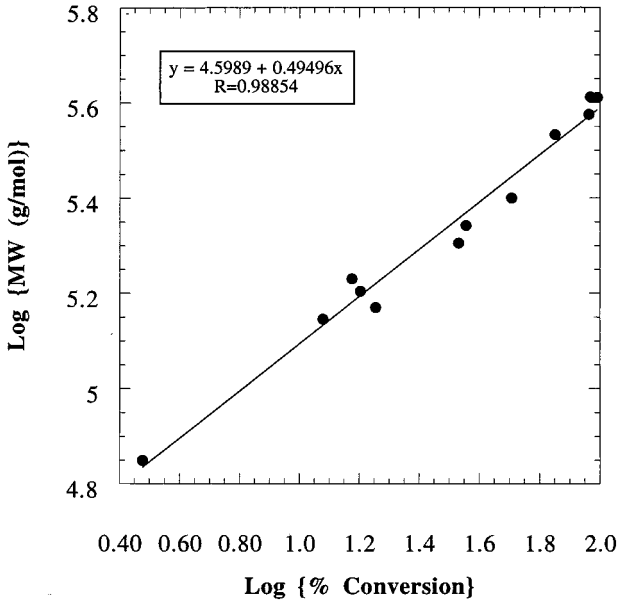

Figure 3. Weight average molecular weight of PMMA versus conversion for polymerizations at 3000 psia and 65 °C.

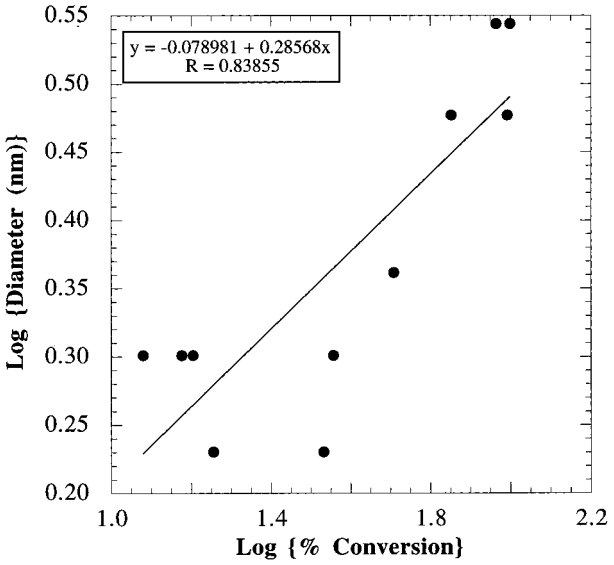

Figure 4. Number average particle size versus conversion for polymerizations at 3000 psia and 65 °C. The uncertainty in average particle size is ± 0.1 μm.

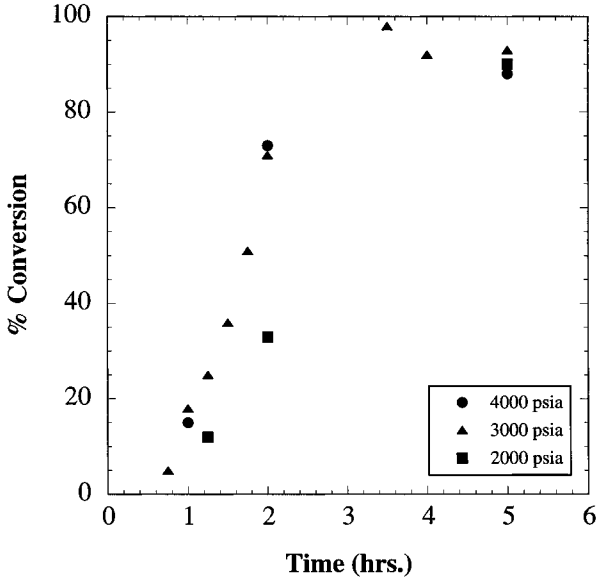

Figure 5. Yield versus time for MMA polymerizations at ~5 wt % PDMS-mMA/MMA and 65 °C for various pressures.

determined for AIBN in pure CO_2 at similar conditions.[26] The presence of a second component (such as monomer) has opposing effects on k_d and f,[26] so it will be assumed for the calculation of k_p that the initiation rate is the same as in pure CO_2. For k_t, a value of 1.4 $\times$ 10^5 L mol^{-1} s^{-1} is given by Barrett[24] for dispersion polymerizations of MMA in n-dodecane at 20% conversion. In dilute solution, k_t has been determined to be 2.7 $\times$ 10^7 L mol^{-1} s^{-1},[24] whereas initially, k_t is 2.5 $\times$ 10^7 L mol^{-1} s^{-1} for bulk MMA polymerizations.[37] The viscosity of the polymer particles is significantly reduced due to the plasticizing effect of CO_2. Because the diffusion coefficient is inversely proportional to viscosity (as dictated by the Stokes−Einstein equation), a value of 2 $\times$ 10^6 L mol^{-1} s^{-1} was estimated for k_t. From eqs 2 and 3 a propagation rate constant for these conditions was determined to be 7.1 $\times$ 10^2 L mol^{-1} s^{-1}, which is in good agreement with values reported in the literature for bulk polymerizations of MMA (5 to 6 $\times$ 10^2 L mol^{-1} s^{-1}).[27,37] This agreement is consistent with Paine's assumption[19] that the bulk value of k_p may be used in the kinetic model for polymerization in the particle phase. Although the main error in the calculation of k_p arises from the estimated value for k_t, $k_p \propto k_t^{1/2}$ and so errors in k_t will produce a minor error in k_p.

Final Particle Number Density and Particle Size. In a dispersion polymerization the final particle size and particle number density are governed by the availability and proficiency of the macromonomer to stabilize the surface generated during the reaction. In the case of a macromonomer stabilizer, the constant C_S in Paine's model is equal to $1/r_1$, where r_1 is the reactivity ratio of monomer to macromonomer. Based on literature data for MMA versus PDMS-MMA, we will assume r_1 is equal to 2.0, and, therefore, C_S is 0.5.[32,33] It is known that PDMS is a poor chain transfer agent. The C_s for siloxane-based molecules in free radical polymerizations is on the order of 2 $\times$ 10^{-5}.[37] It is also known that AIBN, the radical initiator used in this study, is poor at abstracting hydrogen from PDMS.[38] Therefore, all grafting of the macromonomer will only

occur through the methacrylate end group. The value for the macromonomer concentration in eq 4 is based on the number of methacrylate units of the macromonomer in the reaction mixture, determined to be 8.6×10^{-4} M at ~5 wt % PDMS-mMA/MMA.

The radius of gyration of a PDMS chain with a molecular weight of 10 000 g/mol is 2.66 nm in a theta solvent.[37] Because the macromonomer is slightly above or near theta conditions during the particle formation stage, based on its solubility in Figure 1, this value of R_g was used in the Paine model.

The rate constant k_2 represents the diffusional process of collisions of particles and unstabilized nuclei in the reaction medium. Such processes are typically in the range of 10^8 to 10^{10} L mol^{-1} s^{-1}. Paine[19] used a value of 10^9 L mol^{-1} s^{-1} for dispersion polymerizations in liquid media. Based on an order of magnitude lower viscosities for SCFs relative to liquids, a value for k_2 of 10^{10} L mol^{-1} s^{-1} was assumed.

Using an initiator concentration of 0.0105 M (~1 wt % AIBN/MMA), an initial monomer concentration of 1.68 M (~25 wt % MMA/CO_2), and a polymer phase density of 1.0 g mL^{-1}, the final particle size for the latex is 2.9 μm from eq 4, and thus the particle number density is $\sim 2.4 \times 10^{10}$ mL^{-1}. Experimentally, the average particle size of the latex approaches 3.1 μm and the particle number density is $\sim 2.0 \times 10^{10}$ mL^{-1} at the completion of the reaction; these values are in excellent agreement with the predictions of the Paine model. About the same particle size is obtained from the literature value of k_p or the value determined in this study.

Flocculation of the latex can occur for two reasons. As the MMA concentration in the continuous phase decreases, the R_g of the PDMS chains decreases because of poorer solvation. Also, the growing surface area can exceed the surface coverage of the adsorbed stabilizer. The increased stability at 4000 psia relative to lower pressures suggests that solvation of the PDMS chains plays a key role in preventing flocculation.

The Effect of Reaction Pressure. Over the pressure range of 1500 to 4000 psia there was a mild increase in average particle size with pressure. The particles are slightly aggregated at high pressure, but highly coagulated at low pressure, as shown in Figure 6. At 3000 psi and above, the final product was a freely flowing powder. The coagulation indicates that the PDMS tails were not able to sterically stabilize the latex at low pressures or at high conversions when the MMA concentration was low. Increasing the pressure from 3000 to 4000 psia had little effect on yield and molecular weight (Table 1, Table 2). A pressure of 4000 psia is above the phase boundary of the PDMS macromonomer in pure CO_2 (Figure 1), but is not above the theta density for infinite molecular weight PDMS. Even after 5 h reaction time at 4000 psia there did not appear to be any evidence of aggregation from SEM micrographs of latex samples. Polymerizations quenched after 2 h were initially stable to sedimentation, but began to flocculate upon extraction of MMA. In polymerizations quenched after 5 h, the latex rapidly sedimented in the reactor even before extraction. Therefore, although the latex is stabilized to a greater extent at 4000 psia relative to lower pressures, flocculation does ensue as the concentration of MMA is sufficiently reduced. These results agree with previous experimental results for emulsion stabilization in supercritical CO_2[8,9] that suggest that steric stabilization is defined by the theta-point for infinite molecular weight stabilizer tails. These results indicate the danger in inferring stabilization mechanisms from SEM micrographs alone.

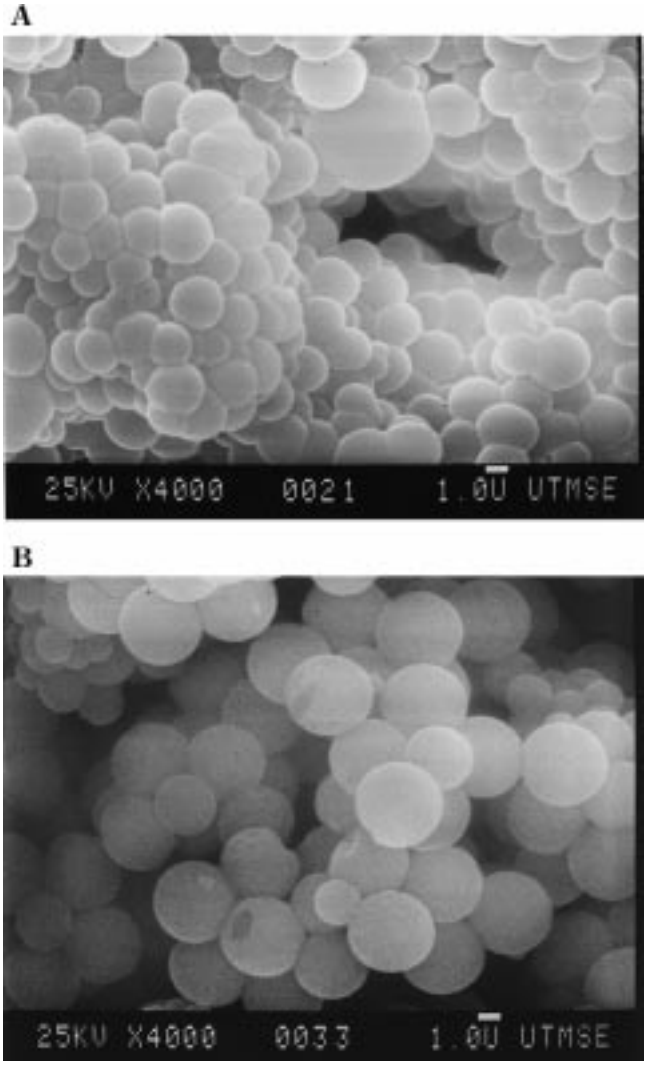

Figure 6. SEM micrographs of PMMA particles produced at 5 h at (A) 1500 psia and (B) 4000 psia. All micrographs are at 4000X magnification.

Table 2. Dispersion Polymerization of MMA in CO_2 at Various Pressures and Times[a]

time (h)	pressure (psia)	yield (%)	M_w ($\times 10^{3}$g/mol) /PDI	product morphology	approximate particle size (μm)/PDI
5	4000	88	365/3.9	uncoagulated	3.3/1.08
2	4000	68	247/4.0	n/a	n/a
1	4000	15	n/a	n/a	n/a
5	3000	93	339/4.0	partially coagulated	3.1/1.11
5	1500	90	481/4.5	coagulated	2.5/1.28
2	2000	34	203/10.9	n/a	n/a
1.25	2000	12	n/a	n/a	n/a

[a] All systems were 25−30 wt % MMA/CO_2, ~5 wt % PDMS-mMA/MMA, ~1 wt % AIBN/MMA, and 65 °C.

Reactions conducted at 2000 psia had a noticeably smaller conversion rate (0.5% min^{-1}) with greater coagulation relative to those at 3000 psia (Figure 6). Dispersions at lower pressures were also found to be flocculated from very early stages of the polymerization, in excellent agreement with part 2.[22] The reduced conversion rate will now be shown to result from the large degree of coagulation of the latex, due to insuf-

ficient stabilization of the PDMS tails as is evident from the phase behavior in Figure 1. A transition from a dispersion polymerization to a precipitation polymerization results from the lack of stabilization.

The flux of MMA into the particle phase may be compared with the rate of conversion to determine when propagation becomes diffusion limited. At 3000 psia, the rate of consumption of MMA was calculated to be $\sim 10^{-6}$ mol s^{-1} per mL of the latex. For this estimation it was assumed that the volume fraction of the particles is 50% polymer, with the remainder being composed of CO_2 and MMA, and that polymerization occurs exclusively within the particle. The diffusion coefficient of monomer in the particle (containing dissolved CO_2) is estimated to be 10^{-6} cm^2 s^{-1} by the extrapolation of data of Berens et al.[35] As a boundary condition for the flux it was assumed that the concentration gradient of MMA went from bulk concentration at the particle surface (~10 wt %) to zero at the center of the particle, at a particle size of 2 μm. The resulting flux is $\sim 10^{-12}$ mol s^{-1} per particle. Because there are of the order of 10^{10} particles per milliliter of latex, the product of the flux per particle and the particle number density indicates that the overall flux of MMA will be of the order of 10^{-2} mol s^{-1} per milliliter of the latex. This value is about four orders of magnitude larger than the rate of consumption. Thus, for stable 2-μm particles, there is sufficient time for monomer diffusion into the particle phase relative to the polymerization rate.

Suppose the particles are not stabilized. An increase in size by two orders of magnitude due to coagulation would reduce the total particle number to $\sim 10^4$. The resulting MMA flux per particle for a 200-μm particle would be $\sim 10^{-10}$ mol s^{-1} and the overall flux would be on the order 10^{-6} mol s^{-1} per milliliter of latex. This flux is the same order of magnitude as the rate of MMA consumption by reaction. From this simple calculation, it can be seen that diffusional restrictions become important for large aggregates.

Polymerizations at 2000 and 1500 psia produced significantly higher molecular weight polydispersities than those at higher pressures. In these cases, multimodal molecular weight distributions were obtained with the lowest molecular weight peak at 1.0 to 1.5 $\times$ 10^4 g mol^{-1}. Similar multimodal distributions were also observed in dispersion polymerizations performed without macromonomer (see below). The unusual distributions are likely caused by two effects: (1) increased contribution of solution polymerization at lower pressures, and (2) trapped PDMS-mMA inside the particles during polymer precipitation, so that it cannot be removed during the CO_2 extraction procedure. These factors are expected to contribute as the solvency of the continuous phase is reduced, both as a result of poorer steric stabilization of the latex and reduced solvation of the macromonomer and polymerized macromonomer by the continuous phase. The reduction of the polymerization rate within the coagulated particle phase due to reduced monomer diffusion results in an increased contribution from polymerization in the solution phase.

There was little change in the average molecular weight of the final product at lower pressures, despite the longer times for complete conversion. The termination rate may also decrease to offset the reduced propagation rate inside the particle. As shown earlier, the large quantity of monomer present initially is cosolvent for PDMS, allowing for stabilization initially during polymerizations even at 1500 psia. The result is similar final particle sizes over a wide range of pressures, indicating the importance of the particle formation stage in the determination of final particle size.

Table 3. Dispersion Polymerization of MMA in CO_2 with Varying Amounts of Stabilizer[a]

conc (wt %) stab./MMA	yield (%)	M_w ($\times 10^3$g/mol) /PDI	product morphology	approximate particle size (μm)/PDI
10.3	88	523/5.1	coagulated	1.7/1.10
6.7	80	n/a	partially coagulated	1.6/1.35
6.3	90	409/4.1	partially coagulated	3.1/1.11
5.8	93	339/4.0	partially coagulated	3.1/1.11
4.8	77	341/4.9	partially coagulated	3.4/1.04
1.5	86	334/3.9	partially coagulated	6.5/1.03
0	71	246/8.5	solid	n/a
0	62	209/11.5	solid	n/a

[a] All systems were PDMS-mMA stabilizer, 25−30 wt % MMA/CO_2, ~1 wt % AIBN/MMA, and at 65 °C.

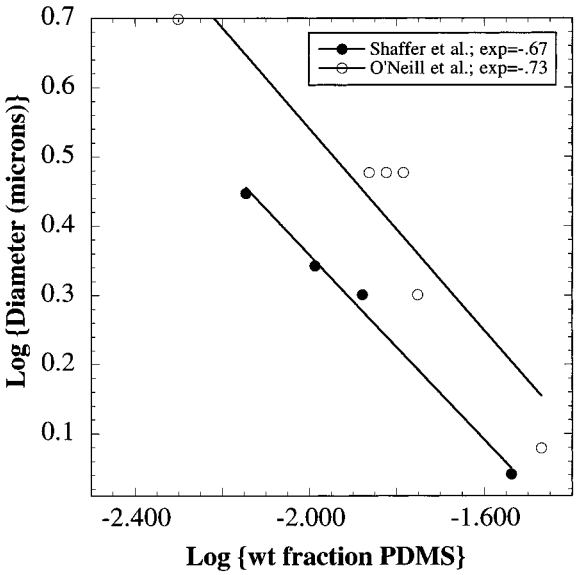

Figure 7. Particle size versus weight fraction macromonomer for polymerizations at 65 °C.

Effect of Stabilizer Concentration. Various amounts of PDMS-mMA (0−10 wt %) were used to study the effect of the macromonomer concentration on latex morphology and molecular weight (Table 3). The slightly smaller particle sizes obtained in Shaffer's study are attributed to a three-fold lower initiator concentration and a 50% lower monomer concentration, both of which will reduce the final particle size.[39] Our results indicate a moderate dependence of both product molecular weight and yield on macromonomer concentration. Regardless of macromonomer concentration, the particles recovered from polymerizations at 3000 psia were somewhat coagulated.

The dependence of particle size on macromonomer concentration is shown in Figure 7 at concentrations >2 wt %. The exponent of the dependence from this study is −0.71, which closely matches the earlier value of −0.67 seen by Shaffer.[15] This exponent is somewhat larger than the value of −0.50 predicted by the Paine model,[19] indicating the amount of surface area stabilized increases slightly more rapidly with stabilizer concentration than predicted.[19] Other studies of nonaqueous dispersion polymerization in hydrocarbons and alcohols have shown that the observed power law dependencies on macromonomer concentration can vary from −0.3 to

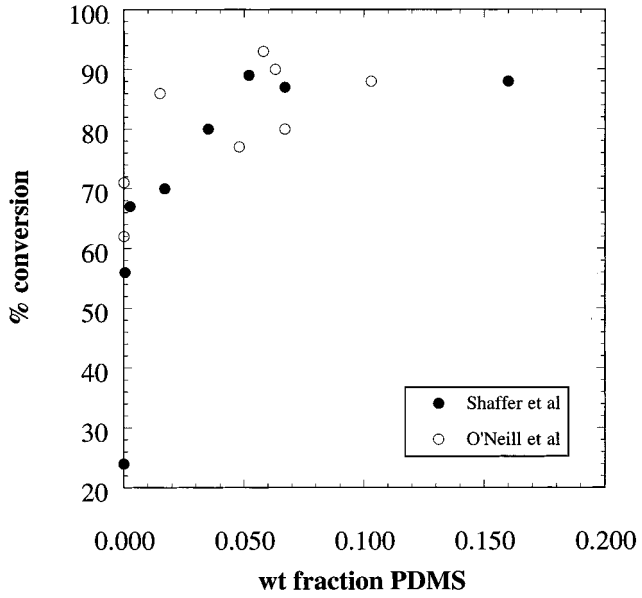

Figure 8. Conversion after 5 h versus weight fraction macromonomer for polymerizations at 65 °C.

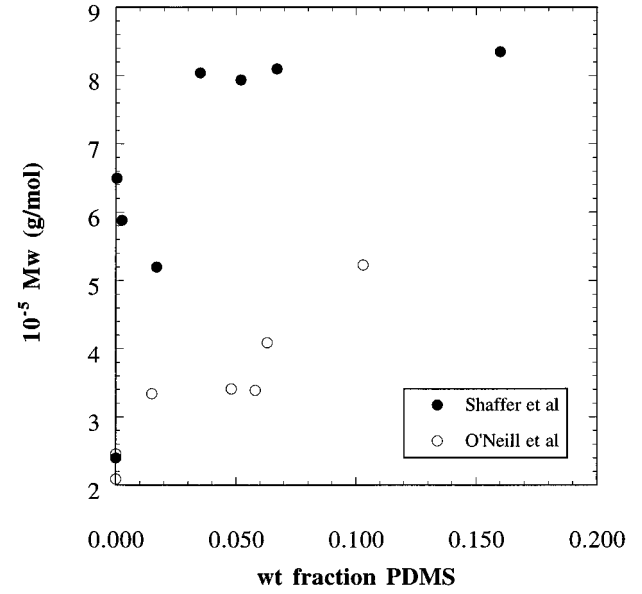

Figure 9. Weight average molecular weight after 5 h versus weight fraction macromonomer for polymerizations at 65 °C. The difference in results is primarily due to the difference in initiator concentrations (see text).

−0.8.[21,39] In part 2,[22] the effect of macromonomer concentration on the particle number density during the particle formation stage is determined with the use of turbidimetry.

A plot of conversion after 5 h versus weight fraction macromonomer (Figure 8) is in good agreement with results in the literature[15] and part 2.[22] The conversion increases gradually with macromonomer concentration. These results are in excellent agreement with part 2.[22] In Figure 9 an increase in the weight average molecular weight is observed with increasing macromonomer concentration. From both conversion and molecular weight data it is evident that increasing wt % of macromonomer up to 2 wt % significantly reduces the contributions from solution phase polymerization.[39,40]

Without stabilizer, the dispersion polymerizations produced coagulated morphologies, with decreased molecular weight and increased polydispersity compared with polymerizations with >2 wt % stabilizer (Table 3). Gel permeation chromatograms of these polymers indicate a multimodal molecular weight distribution, with a primary peak around 1 to 1.5 × 10^4 g mol^{-1} and a secondary peak around 2 × 10^4 g mol^{-1} of approximately half the size of the primary peak. Frequently a third peak was also seen. This third peak was much smaller than the previous two, appearing as a high molecular weight shoulder on the main peak. Recent studies have shown that three distinct molecular weight populations may exist in free radical polymerizations,[41] corresponding to the three molecular weights peaks observed in this study. Although the exact cause of the multimodal profiles in GPC chromatograms is not known, they were obtained only in reactions at low pressures or without macromonomer.

Conclusions

The mechanism of stabilization is complicated because of changes in the composition and solvent quality of the continuous phase and the availability and conformation of the stabilizer. Because CO_2 is a mediocre solvent for PDMS, the dispersions flocculate before polymerization is complete due to the loss of solvation by monomer, unlike the case for conventional dispersion polymerization.

Analysis of the chronology of molecular weight, particle size, product morphology, and polymerization rate indicates that the main locus of polymerization is the particle phase, and that for the majority of the polymerization, no new particles are formed because particle volume increases directly with conversion. The final particle size and number density determined from the model of Paine[19] agree with the measured values, although limitations of the model are apparent (see part 2).

The time period over which the dispersion remained stable is extended by increasing pressure. At low pressures (e.g., ∼2000 psia), the dispersion flocculates and coagulates very early. There exists both a minimum pressure (∼3000 psia) and stabilizer concentration (∼2 wt % stabilizer/monomer) below which polymerization rates are greatly reduced and particles are highly coagulated. Above 3000 psia, particle size is only mildly dependent on pressure, which is in agreement with previous studies.[12,15] The high concentrations of monomer initially present in the reaction enable stabilization of the dispersion during the critical particle formation stage even at very low pressures. Thus, small, yet highly coagulated, particles and high molecular weights are observed at low pressure. In contrast, stabilizer concentration has a strong effect on particle size.

Acknowledgment. We acknowledge support from the Separations Research Program at the University of Texas, the National Science Foundation, the Department of Energy, and Air Products and Chemicals. Mark O'Neill acknowledges support from the Natural Sciences and Engineering Research Council of Canada. In addition, we thank ISCO Corporation for the donation of a high-pressure syringe pump. The support of these agencies does not constitute an endorsement of the views expressed in this article. Special thanks to Dr. Simon Mawson for technical support on SEMs, to Sona Maniar for particle size analysis of SEM micrographs, and to Brian Hanley and Dennis Nagy of Air Products

and Chemicals, Inc. for performing molecular weight analyses.

References and Notes

(1) Fulton, J. L.; Smith, R. D. *J. Phys. Chem.* **1988**, *92*, 2903−2907.
(2) Johnston, K. P.; McFann, G. J.; Lemert, R. M. In *Supercritical Fluid Science and Technology*; Johnston, K. P., Penninger, J. M. L., Ed.; ACS Symposium Series 406, American Chemical Society: Washington, DC, 1989; pp 140−164.
(3) McFann, G. J.; Johnston, K. P. *J. Phys. Chem.* **1991**, *95*, 4889−4896.
(4) Peck, D. G.; Johnston, K. P. *J. Phys. Chem.* **1991**, *95*, 9549−9556.
(5) Bartscherer, K. A.; Renon, H.; Minier, M. *Fluid Phase Equilibria* **1995**, *107*, 93−150.
(6) McFann, G. J.; Johnston, K. P. In *Microemulsions: Fundamental and Applied Aspects*; Kumar, P., Ed.; Marcel Dekker: New York, in press.
(7) Peck, D. G.; Johnston, K. P. *J. Phys. Chem.* **1993**, *97*, 5661−5667.
(8) O'Neill, M. L.; Yates, M. Z.; Harrison, K. L.; Johnston, K. P.; Canelas, D. A.; Betts, D. E.; DeSimone, J. M.; Wilkinson, S. P. *Macromolecules* **1997**, *30*, 5050−5059.
(9) Yates, M. Z.; O'Neill, M. L.; Johnston, K. P.; Webber, S.; Canelas, D. A.; Betts, D. E.; DeSimone, J. M. *Macromolecules* **1997**, *30*, 5060−5067.
(10) DeSimone, J. M.; Maury, E. E.; Menceloglu, Y. Z.; McClain, J. B.; Romack, T. J.; Combes, J. R. *Science* **1994**, *265*, 356.
(11) Adamsky, F. A.; Beckman, E. J. *Macromolecules* **1994**, *27*, 312−314.
(12) Hsiao, Y.-L.; Maury, E. E.; DeSimone, J. M.; Mawson, S.; Johnston, K. P. *Macromolecules* **1995**, *28*, 8159−8166.
(13) Canelas, D. A.; Betts, D. E.; DeSimone, J. M. *Macromolecules* **1996**, *29*, 2818−2821.
(14) Kapellen, K. K.; Mistele, C. D.; DeSimone, J. M. *Macromolecules* **1996**, *29*, 495−496.
(15) Shaffer, K. A.; Jones, T. A.; Canelas, D. A.; DeSimone, J. M.; Wilkinson, S. P. *Macromolecules* **1996**, *29*, 2704−2706.
(16) Lepilleur, C.; Beckman, E. J. *Macromolecules* **1997**, *30*, 745−756.
(17) DeSimone, J. M.; Guan, Z.; Elsbernd, C. S. *Science* **1992**, *257*, 945.
(18) O'Neill, M. L.; Cao, Q.; Fang, M.; Johnston, K. P. *Ind. Eng. Chem. Res.*, in press.
(19) Paine, A. J. *Macromolecules* **1990**, *23*, 3109−3117.
(20) Lacroix-Desmazes, P.; Guyot, A. *Macromolecules* **1996**, *29*, 4508−4515.
(21) Kawaguchi, S.; Winnik, M. A.; Ito, K. *Macromolecules* **1995**, *28*, 1159−1166.
(22) O'Neill, M. L.; Yates, M. Z.; Johnston, K. P.; Smith, C. D.; Wilkinson, S. P. *Macromolecules* **1998**, *31*, 2848.
(23) Barrett, K. E. J. *Dispersion Polymerization in Organic Media*; John Wiley and Sons: New York, 1975.
(24) Barrett, K. E. J.; Thomas, H. R. *J. Polym. Sci., Part A-1* **1969**, *7*, 2621−2650.
(25) Croucher, M. D.; Winnik, M. A. In *An Introduction to Polymer Colloids*; Candau, F., Ottewill, R. H., Eds.; Kluwer Academic: 1990; pp 35−72.
(26) Guan, Z.; Combes, J. R.; Menceloglu, Y. Z.; DeSimone, J. M. *Macromolecules* **1993**, *26*, 2663−2669.
(27) Odian, G. *Principles of Polymerization*, 3rd ed.; John Wiley & Sons: New York, 1991.
(28) Condo, P. D.; Paul, D. R.; Johnston, K. P. *Macromolecules* **1994**, *27*, 365−371.
(29) O'Neill, M. L.; Handa, Y. P. In *Assignment of the Glass Transition, ASTM STP 1249*; Seyler, R. J., Ed.; American Society for Testing and Materials: Philadelphia, 1994; pp 165−173.
(30) Handa, Y. P.; Kruus, P.; O'Neill, M. *J. Polym. Sci., Part B: Polym. Phys.* **1996**, *34*, 2635−2639.
(31) de Gennes, P. G. *Adv. Colloid Interface Sci.* **1987**, *27*, 189−209.
(32) Tsukahara, Y.; Hayashi, N.; Jiang, X.-L.; Yamashita, Y. *Polym. J.* **1989**, *21*, 377−391.
(33) Cameron, G. G.; Chisolm, M. S. *Polymer* **1985**, *26*, 437−442.
(34) Chillura-Martino, D.; Triolo, R.; McClain, J. B.; Combes, J. R.; Betts, D. E.; Canelas, D. A.; DeSimone, J. M.; Samulski, E. T.; Cochran, H. D.; Londono, J. D.; Wignall, G. D. *J. Mol. Struct.* **1996**, *383*, 3−10.
(35) Berens, A. R.; Huvard, G. S. *Interaction of Polymers with Near Critical Carbon Dioxide*; Berens, A. R., Huvard, G. S., Eds.; American Chemical Society: Washington, D.C., 1989; Vol. 406, pp 207−223.
(36) Sandler, S. J.; Karo, W. *Polymer Synthesis*; Academic: New York, 1996; Vol. 29-III.
(37) Brandrup, J.; Immergut, E. H. *Polymer Handbook*, 3rd ed.; John Wiley and Sons: New York, 1989.
(38) Pelton, R. H.; Osterroth, A.; Brook, M. A. *J. Colloid Interface Sci.* **1990**, *137*, 120−127.
(39) Winnik, M. A.; Croucher, M. D. In *Future Directions in Polymer Colloids*, El-Aasser, M. S., Fitch, R. M., Eds.; Martinus Nijhoff: Boston, 1987; Vol. 138; pp 209−228.
(40) Shen, S.; Sudol, E. D.; El-Aasser, M. S. *J. Polym. Sci., Part A: Polym. Chem.* **1994**, *32*, 1087−1100.
(41) Cunningham, M. F.; Mahabadi, H. K. *Macromolecules* **1996**, *29*, 835−841.

MA971314I